PROCEEDINGS. Twenty-Third Workshop on Geothermal Reservoir Engineering
Stanford University, Stanford, California, January 26-28, 1998
SGP-TR-158

Simulating Fenton Hill HDR Test Results Using the GEOTH3D Code

Takeshi Yamamoto[1], Yuzuru Eguchi[1], Kouichi Kitano[1]
Donald Brown[2], Dave Duchane[2], Michael Fehler[2], Hiroshi Ohnishi[3]
[1] Central Research Institute of Electric Power Industry, 1646 Abiko-shi, Chiba-ken 270-11 JAPAN t-yama@criepi.denken.or.jp, eguchi@criepi.denken.or.jp
[2] Los Alamos National Laboratory, USA
[3] Denryoku Computing Center, Japan

ABSTRACT

At the Fenton Hill hot dry rock (HDR) Test Site, the Long-Term Flow Test (LTFT) of the deeper reservoir was conducted from April 1992 through April 1993, following a multi-year period of reservoir pressurization at 15.6 MPa. At an injection pressure of 27.3 MPa, the steady-state fluid recovery at the production well (not including the additional production flow up the annulus at the injection well) was 80% at a backpressure of 12.4 MPa and 73% at a backpressure of 15.2 MPa.

The reservoir simulation code GEOTH3D, a model based on an assumed relationship between the distribution of permeability and the corresponding distribution of acoustic emissions (AE) throughout the pressure-stimulated reservoir region, was applied to the LTFT data to determine the applicability of this code to a second HDR reservoir. The principal model output, the percent recovery of fluid at the production well under two different steady-state operating conditions, was obtained by specifying the surface injection pressure and backpressure as boundary conditions. At an injection pressure of 27.3 MPa, the computed fluid recoveries were 81 % and 75 %, respectively, at the two different backpressure levels of 12.4 MPa and 15.2 MPa, in good agreement with the measured LTFT results. Therefore, the proposed three-dimensional reservoir modeling method, coupling the permeability values to the AE data, appears to be very effective in simulating the Fenton Hill HDR reservoir.

INTRODUCTION

GEOTH3D (Yamamoto et al., 1995) is a numerical model that simulates three-dimensional fluid- and heat-transport in porous media, and is used to model the behavior of a hot dry rock (HDR) reservoir. It is composed of two equations for mass and energy balance (based on Darcy's law), which are discretized by three-dimensional finite difference approximations with fully implicit Newton-Raphson treatment of the nonlinear terms.

We determined the three-dimensional physical properties of the numerical reservoir by using permeability tests to relate the 3-D permeability distribution to the 3-D AE (i.e., microseismic) data. GEOTH3D can be used to estimate both reservoir fluid recovery and temperature changes.

The results of the Ogachi site simulation showed good agreement with the experimental data, and led to the conclusion that the proposed reservoir modeling procedure was effective, at least for the Ogachi Site (Yamamoto et al., 1996).

LANL and CRIEPI have been collaborating in applying thermal-hydraulic analysis codes to each other's HDR systems, in order to evaluate the versatility and limitations of these codes, and to improve their capabilities. In this paper we present the results obtained fiom applying the CRIEPI simulation code, GEOTH3D, to the steady-state LTFT data from Fenton Hill. In a subsequent study, we will apply the LANL HDR reservoir analysis code (GEOCRACK, developed by Prof. Daniel Swenson at Kansas State University) to the Ogachi test data.

NUMERICAL METHOD

Constitutive Relationships

Based on the following assumptions (Faust et al., 1979), we developed mathematical models for energy balance, and for mass and momentum balance (using Darcy's law):

1) Capillary pressure effects are neglected.
2) Water, steam, and rock are thermally equilibrated.
3) The reservoir fluid is either single phase or two phase.
4) Relative permeability is only a function of liquid volume saturation rate; hysteresis is neglected.
5) Viscosity is considered a function of both pressure and temperature.
6) Porosity is a linear function of pressure.
7) Rock density, reservoir thickness, and the intrinsic permeability tensor are arbitrarily given in three-dimensional space.

8) The mass and energy source terms represent the amount of mass and enthalpy due to source-sink capacity.
9) Rock enthalpy is a linear function of temperature.

RESERVOIR MODEL

Finite-Difference Blocks

We described the three-dimensional conceptual Fenton Hill reservoir model as a porous medium divided into finite-difference blocks. The computational area was 3000 m (in E-W direction) x 3000 m (in S-N direction) x 2500 m (in depth). We assigned the same size to all the finite-difference blocks: 20 m x 20 m x 20 m. The number of blocks was 150 (E-W) x 150 (S-N) x 125 (depth), totaling 2,812,500.

Injection and Production Points

The injection and production wellbores were named EE-3A and EE-2A, respectively. On the injection (EE-3A) side, the openhole interval ranged fiom 3485 m to 3730 m (depth measured along the wellbore). The interval, measured in true vertical depth (TVD), ranged fiom 3415.5 m to 3657 m. Hence, we set the modeled reservoir injection interval from 3430 m to 3650 m (TVD).

On the production (EE-2A) side, the openhole interval ranged fiom 3283 m to 3734 m. However, the set of 8 producing joints ranged fiom only 3307 m to 3658 m (depth along the wellbore). Brown (1994) showed a number of flowing joint intersections with the wellbore based on a production temperature log across the producing interval in EE-2A. Four principal intersections were located at 3276.6 m, 3349.8 m, 3450.3 m and 3608.8 m (TVD). Hence, we set the production interval from 3270 m to 3610 m (TVD). Figure 1 shows the two wellbore trajectories near the injection and production intervals.

Application of AE Data

The majority of the reservoir was initially formed at an average injection pressure of 48 MPa during the massive hydraulic fracturing test in December 1983. The reservoir was then extended to the south and east at injection pressures up to 32 MPa during the initial 30-day flow test in mid-1986. The volume of the stimulated region, as determined fiom the envelope of AE events defining the pressure-stimulated reservoir (the seismic volume), was about 130 million m^3. There appears to be a linear relationship between reservoir volume and volume of injected fluid as determined fiom the AE event-location data fiom the massive hydraulic fracturing test (Brown, 1995).

In applying GEOTH3D for reservoir simulation, we needed the microseismic event locations and magnitudes to obtain the cumulative magnitude for each finite difference block (Yamamoto et al., 1995). Unfortunately, the magnitudes of the AE were not available at the Fenton Hill site. Hence, when applying the reservoir modeling procedure, we assumed that each AE event emitted the same energy.

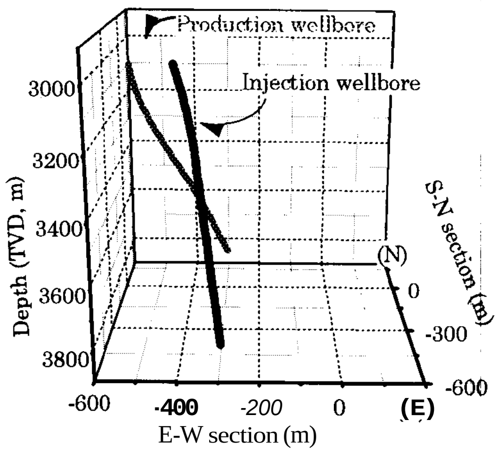

Fig. 1 Wellbore trajectories around injection and production intervals

There were two assumptions in the reservoir modeling procedure:

1] Hydraulic flow in the fractured rock can be represented by the flow through a porous media.
[2] Mean permeability values for each block are proportional to cumulative magnitude values of the AE (summation of the number of AE events, in this study).

Under these assumptions, the numerical reservoir was formulated by the following procedure:

1) Divide a computational area into finite difference blocks. (20-m cubes, in this study)
2) Sum up the number of AE events that occurred in each block, defined as C_1.
3) Pick the eighteen blocks, bordering the six faces and twelve edge lines of the core block, as shown below.

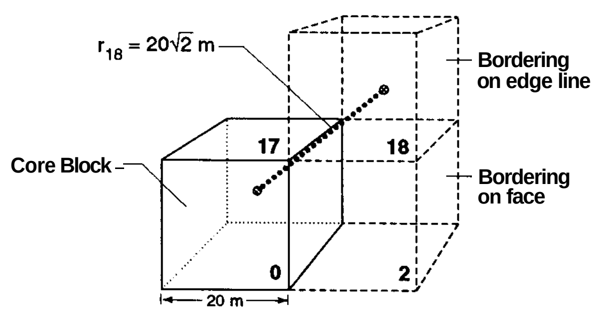

4) Apply the weighted averaging method among the eighteen bordering blocks and the core block. The distance between the center of the core block and that of the bordering block was set as r_i, while r_0, the distance for a core block itself, was set at unity. We assumed the seismic area was equal to or smaller than 20 m (segmental length) multiplied by the square root of 2. We applied the weighted parameter "w_l" to obtain the averaged number of AE events, "C_{ijk}". This weighted averaging method is usually used in image processing.

$$C_{i,j,k} = \sum_{l=0}^{18} w_l C_l$$

$$w_l = \frac{\frac{1}{r_l^2}}{\sum_{i=0}^{18} \frac{1}{r_i^2}}, \quad \frac{1}{r_0} = 1, \quad r = 20, \quad 20\sqrt{2} \ \text{(m)}$$

In the above equation, C_l is the number of AE events occurring in a local block (no. 1).

5) Apply Laplacian Filtering method to the three-dimensional map of C_{ijk}.

6) Classify the cumulative number of AE events into five grades, from I to V.

Permeability Data

The following calculations show how we estimated *in situ* permeability around the injection wellbore, especially around the bottom part of the wellbore (fractured zone).

If we assume the flow is laminar, the flow rate through a single joint (Q_l) can be described as follows:

$$Q_l = \frac{t^3}{12} \cdot \frac{1}{\eta} \cdot \frac{\partial p}{\partial y} \cdot b \tag{1}$$

Darcy flow (Q_d) between two neighboring joints can be obtained as follows:

$$v = \frac{K}{\eta} \cdot \frac{\partial p}{\partial y} \tag{2}$$

$$\therefore \ Q_d = hbv = \frac{Khb}{\eta} \cdot \frac{\partial p}{\partial y} \tag{3}$$

Hence, permeability (K) can be obtained by equations (1) and (3), $Q_l = Q_d$, as follows:

$$K = \frac{t^3}{12h} \tag{4}$$

In the above equations, t is joint aperture, h is joint spacing, b is joint width, Q_l and Q_d are fluid flow rates, v is fluid velocity and η is fluid viscosity.

The mean joint aperture in the Fenton Hill Phase II reservoir was estimated to be 0.2 mm at the point where the joints are ready to jack open (i.e., when the internal fluid pressure just equals the normal joint closure stress). The measured joint spacing for the fluid conductive joints, based on wellbore temperature logs and joint orientations, was estimated to be more than 2 m and less than 10 m.

Hence, the permeability around the injection wellbore can be calculated by applying the equation (4), to vary from 6.7×10^{-14} m^2 to 3.3×10^{-13} m^2. Taking into account the actual crack undulation, we adopted 5×10^{-14} m^2 as the highest permeability in this study,

The measured permeability of the matrix rock (not including joints) in the Phase II reservoir region was 0.1 micro darcy(1×10^{-17} m^2). Hence, in this study, we set the lowest permeability in the modeled reservoir at 1×10^{-17} m^2.

Three-dimensional Permeability Map

Each of the five grades of permeability was allocated to the blocks according to the cumulative number of AE events (CN). The three-dimensional permeability map was then obtained from the 3-D CN distribution in the reservoir.

Boundary Conditions

In plan view, the modeled reservoir region was extended considerably beyond the margin of the microseismically active region to minimize computational problems. The margin for the Fenton Hill HDR reservoir was set as about 700 m (linearly 35 blocks) at each side, with a computational area of 3000 m x 3000 m.

The boundary conditions for the fluid and energy flow equations at the four vertical sides and two horizontal sides of the modeled region were set as constant pressure and temperature, the same as the initial conditions (that is, boundary permeability).

P = const., T = const.

We simulated two steady-state circulating conditions during the LTFT at Fenton Hill. The surface injection and production pressures were held constant for each steady-state computational run, providing estimates of the hydraulic flow rates. The downhole pressures across the injection and production intervals were determined by adding the hydraulic head to the observed wellhead backpressures. The injection wellhead pressure was set at 27.3 MPa, and the two states of production wellhead pressure were set at 12.4 MPa and 15.2 MPa, respectively.

Rock Properties

Physical rock properties at the Fenton Hill site were as follows:

Thermal Conductivity:	2.7 W/m-K
Density:	2.7 g/cm^3
Heat Capacity:	0.8 joules/g-K

RESULTS

Parameter Survey

We used a parameter survey to determine how to divide the five grades of CN and how to allocate the gradations in permeability in order to obtain a number of three-dimensional reservoir maps.

For input data, we needed injection pressure and production pressure. We set these at 27.3 MPa and 12.4 MPa, respectively, corresponding to one steady-state operating condition maintained during the LTFT.

The parameters were set as follows: [K stands for permeability (m^2) and CN stands for cumulative numbers of AE events obtained after the three-dimensional smoothing. For example, [0,2) stands for a range of CN greater than or equal to 0 and less than 2.]

Case-1:

CN	[0,2)	[2,5)	[5,10)	[10,25)	[25,500)
K	$1x10^{-17}$	$1x10^{-16}$	$1x10^{-15}$	$5x10^{-15}$	$5x10^{-14}$
grade	I	II	III	IV	V

Case-2:

CN	[0,2)	[2,5)	[5,10)	[10,25)	[25,500)
K	$1x10^{-17}$	$1x10^{-16}$	$1x10^{-15}$	$2x10^{-15}$	$1x10^{-14}$
grade	I	II	III	IV	V

Case-3:

CN	[0,2)	[2,5)	[5,10)	[10,25)	[25,500)
K	$1x10^{-17}$	$1x10^{-16}$	$1x10^{-15}$	$5x10^{-15}$	$1x10^{-14}$
grade	I	II	III	IV	V

Case-4:

CN	[0,2)	[2,5)	[5,10)	[10,25)	[25,500)
K	$1x10^{-17}$	$1x10^{-16}$	$1x10^{-15}$	$5x10^{-14}$	$2x10^{-14}$
grade	I	II	III	IV	V

Case-5:

CN	[0,2)	[2,5)	[5,10)	[10,25)	[25,500)
K	$1x10^{-17}$	$1x10^{-16}$	$1x10^{-15}$	$2x10^{-15}$	$5x10^{-15}$
grade	I	II	III	IV	V

Case-6:

CN	[0,2)	[2,5)	[5,10)	[10,30)	[30,500)
K	$1x10^{-17}$	$1x10^{-16}$	$1x10^{-15}$	$5x10^{-15}$	$5x10^{-14}$
grade	I	II	III	IV	V

Case-7:

CN	[0,2)	[2,5)	[5,10)	[10,30)	[30,500)
K	$1x10^{-17}$	$1x10^{-16}$	$1x10^{-15}$	$2x10^{-15}$	$1x10^{-14}$
grade	I	II	III	IV	V

Case-8:

CN	[0,2)	[2,5)	[5,10)	[10,30)	[30,500)
K	$1x10^{-17}$	$1x10^{-16}$	$1x10^{-15}$	$5x10^{-15}$	$2x10^{-14}$
grade	I	II	III	IV	V

Figure 2 shows CN divided into five grades. Both axes were divided logarithmically. We performed a sensitivity analysis by changing the range of the upper ranks IV and V. Simultaneously, the upper ranks of permeability were changed, as shown above for Case-1 to Case-8.

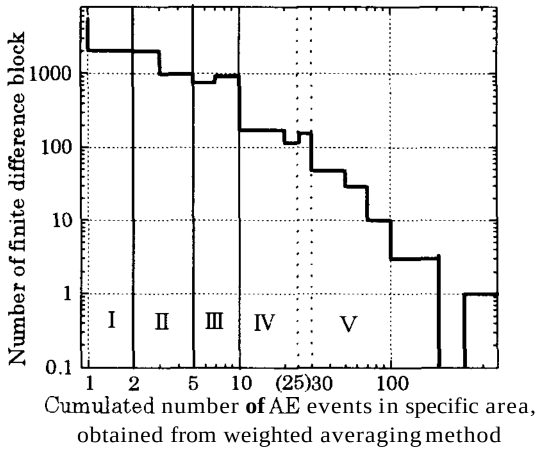

Fig.2 CN divided into five grades

Table-1 shows the results for these calculations. For comparison, the steady-state injection and production values during the LTFT were 7.14 l/s and 5.71 l/s, respectively. .

Table-1: Simulated Flow Rates and Recovery (Injection: 27.3 MPa; Production: 12.4 MPa)

	Injection (l/s)	Production (l/s)	Recovery (%)
Case-1	22.3	20.8	93.2
Case-2	9.33	7.86	84.2
Case-3	13.0	11.5	88.3
Case-4	16.3	14.8	90.6
Case-5	7.73	6.26	81.0
Case-6	15.2	13.7	90 2
Case-7	7.59	6.14	80.9
Case-8	13.6	11.9	88.8
Field data	7.14	5.71	80.0

For the numerical reservoir in Case-1, the high flow rates at both wellbores and the high recovery suggested that the modeled impedance between the wellbores was too low. More realistic values of flow rates and recovery for the numerical reservoir were obtained by applying the parameters of Case-5 and Case-7. These two cases gave the best approximations to the actual measured data for Fenton Hill.

Parameter Verification

The second set of flow test data, obtained during the LTFT at an injection pressure of 27.3 MPa, and the higher backpressure of 15.2 MPa, were applied to the simulation to verify the proposed parameters. For this case, the backpressure at the production wellhead was higher than the first condition of 12.4 MPa *(see* above). The measured injection and production flows rate data were 7.33 l/s and 5.34 l/s. The recovery was 72.9%, about 10% lower than that for the previous steady-state condition.

Table-2 shows the results of the calculations for parameter verification. The two sets of parameters, Case-5 and Case-7, again showed results most comparable to the field data. We therefore chose these parameter sets (Case-5 and Case-7) to be the most appropriate parameters for modeling the numerical reservoir. The permeability for the most fractured region, where the connectivity between the wellbore and reservoir was dramatically improved, was estimated to be about 5×10^{-14} m^2 (see above). In examining the results of our permeability estimations, we chose grade-V of Case-7, 1×10^{-14} m^2, as the most reasonable and practical value for our reservoir modeling.

Table-2 Simulated Rates and Recovery
(Injection: 27.3 MPa; Production: 15.2 MPa)

	Injection (l/s)	Production (l/s)	Recovery (%)
Case-1	18.3	16.7	90.9
Case-2	7.75	6.15	79.3
Case-3	10.8	9.11	84.7
Case-4	13.4	11.8	87.7
Case-5	6.45	4.85	75.3
Case-6	12.5	10.9	87.0
Case-7	6.32	4.75	75.1
Case-8	11.0	9.34	85.2
Field data	1.33	5.34	72.9

Numerical Reservoir

The numerical reservoir was represented by five grades of permeability in a three-dimensional contour map. Figures 3, **4**, and 5 apply Case-7 parameters to show the horizontal cross-section contour maps of the modeled reservoir. The depths of the cross-sections were 3390 m, 3490 m, and 3590 m (TVD). These maps contained the open-hole intervals of the wellbores.

Permeability grades IV and V (2×10^{-15} m^2 and 1×10^{-14} m^2, respectively) indicate the high permeability area. The concentration of the high-permeability contour blocks surrounding and between the wellbores most probably controls both the fluid flow rates and recoveries in these regions of the reservoir.

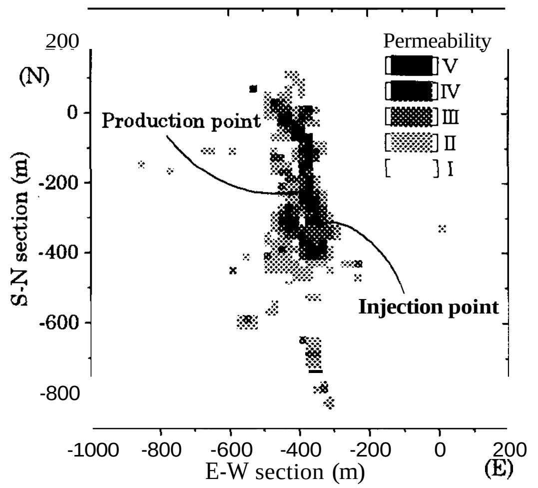

Fig. 3 Permeability at 3390 m depth (TVD)

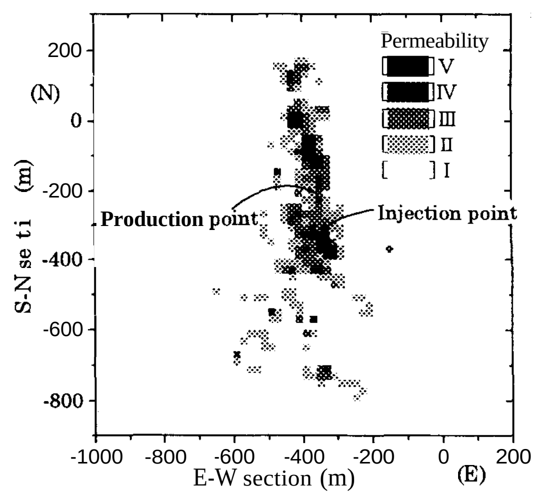

Fig. 4 Permeability at 3490 m depth (TVD)

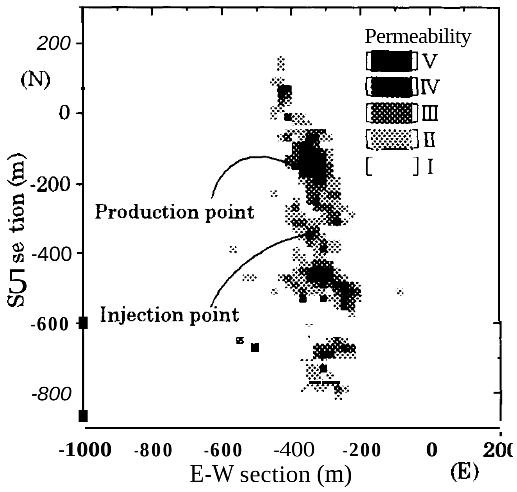

Fig. 5 Permeability at 3590 m depth (TVD)

Connectivity Between the Wellbores

Most of the injected fluid (about *65%)* entered the numerical reservoir in the wellbore interval between **3430** m and **3470 m (TVD).**

Then, **77%** of the recovered water flowed into the production wellbore between **3410** m and **3450 m** (TVD). This indicated that the hydraulic impedance between the wellbores at this section was much lower than at the other sections.

Both wellbores came close to each other at around a depth of **3400-m,** as shown in Figure 1. The horizontal permeability map (see the **3390-m** depth section in Figure **3)** shows the **area** between the wellbores at this depth contained more IV- and V-grade permeability blocks than the other two horizontal sections (i.e., Figures **4** and 5). Hence, the horizontal section around **3400** m (TVD) provided both high fluid recovery and low hydraulic impedance.

Figures 6 and 7 show the pressure contours and Darcy velocity vector distributions at **3410-m** and 3430-m TVD, respectively. The pressure contour interval is 1 MPa. An effective injection point existed at **3430-m** TVD, and an effective production point existed at **3410-m** TVD.

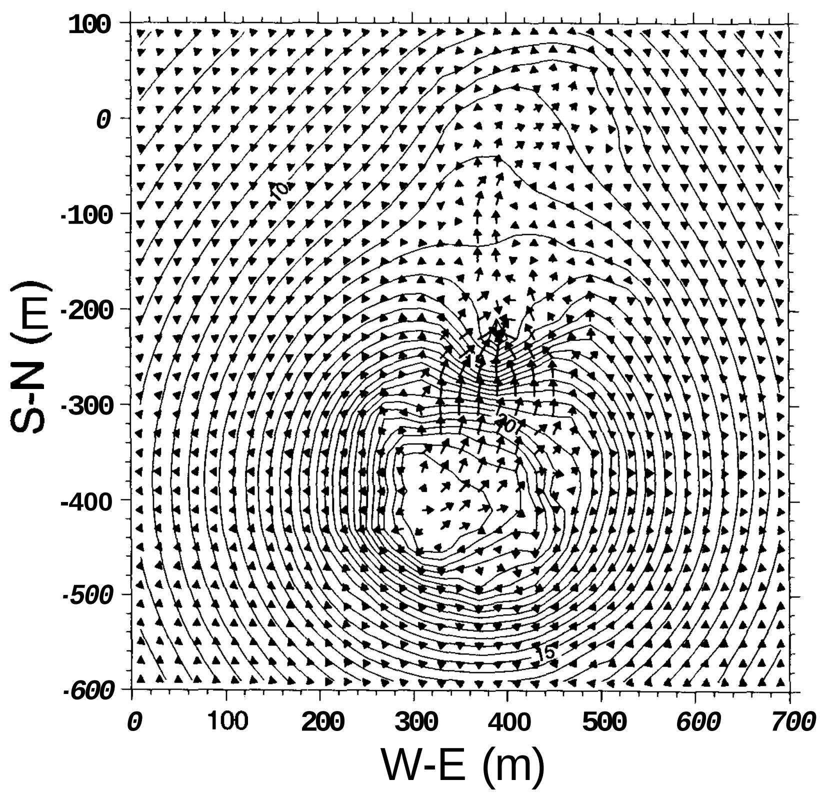

Fig. 6 Pressure contour and Darcy velocity vector at 3410 m TVD

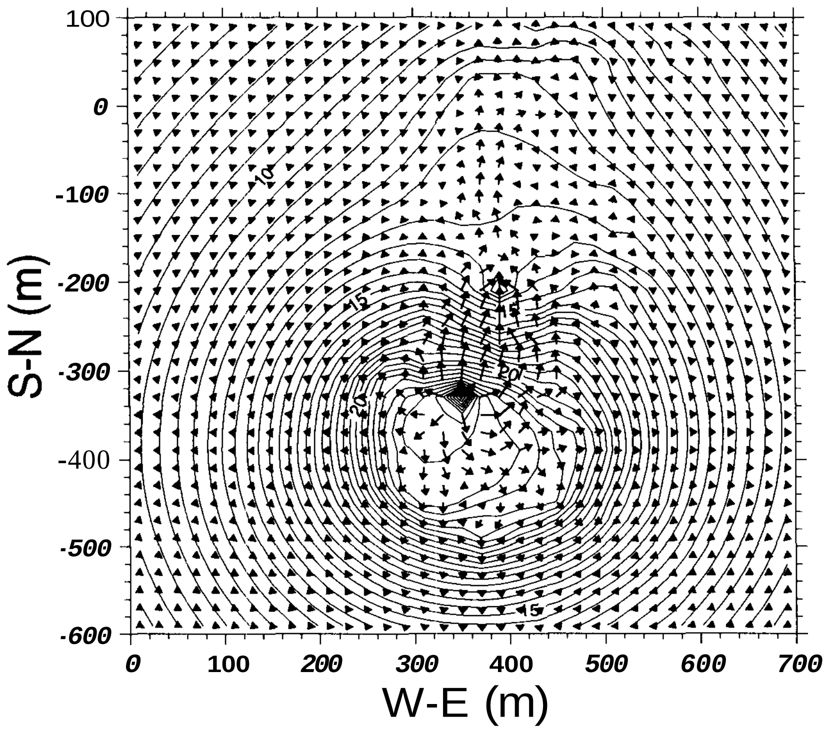

Fig. 7 Pressure contour and Darcy Velocity vector at 3430 m TVD

CONCLUSIONS

Application of GEOTH3D to the Fenton Hill site has shown the following:

- The results of simulated fluid recovery were in good agreement with experimental data.
- A realistic threedimensional reservoir model could be obtained by applying the distribution of AE data to approximate the range of permeabilities.
- Permeability values for both the matrix rock at the reservoir periphery and for the much more permeable fractured area around and between the wellbores are essential in reservoir modeling.
- It would have been useful to use more than two hydraulic circulation conditions to cross-check the relation between the cumulative number of AE and the permeability.

REFERENCES

Brown, D. (1994), "Summary of Recent Flow Testing of the Fenton Hill HDR Reservoir," Proc. 19th Workshop on Geothermal Reservoir Engineering, Stanford Univ., Stanford, CA, Jan. 18-20, 1994, SGP-TR-147, pp. 113-116.

Brown, D. (1995), "The US Hot Dry Rock Program - 20 Years of Experience in Reservoir Testing," Proceedings, World Geothermal Congress 1995, pp. 3607-2611.

Faust, C.R. and Mercer, J.W. (1979), "Geothermal Reservoir Simulation 1. Mathematical Models for Liquid- and Vapor- Dominated Hydrothermal Systems," Water Resources Research Vol. 15, no. 1, pp. 23-30.

Yamamoto, T., Fujimitsu, Y. and Ohnishi, H. (1995), "Hot Dry Rock Reservoir 3D Simulation of the Ogachi Site," Geothermal Resources Council Transactions, Vol. 19, pp. 287-294.

Yamamoto, T., Kitano, K., Tanaka, N. and Ohnishi, H. (1996), "Hot Dry Rock Reservoir 3D Simulation of the Ogachi Site II", Geothermal Resources Council Transactions, Vol. 20, pp. 467-474.